

# Latitudinal Profile of the Solar Wind Velocity – A Prediction for the Coming Solar Maximum

**Bala Balachandran and Silvia Bravo**

Instituto de Geofísica

Universidad Nacional Autónoma de México

Coyoacan, D.F., 04510

We present the results of the latitudinal gradient of solar wind velocity at the source surface obtained using the potential field source surface model of Hoeksema and the relation between the magnetic flux expansion factor and the solar wind velocity for individual Carrington rotations during the previous solar maximum, i. e., 1989–90 and the present year 1999. Using these profiles, the latitudinal gradient for the next maximum in 2000 is predicted. Also, a comparison with the results of the NOAA/SEC daily updated version of the Wang and Sheeley model as well as IPS data is presented.

## 1 A Little Background

Wang and Sheeley (1994) obtained an inverse correlation between the flux expansion factor of the magnetic field and the solar wind velocity observed at earth. The expansion factor,  $f$ , is the factor by which the magnetic flux tube expands between the photosphere and the source surface (at  $2.5 R_{\odot}$ ). Mathematically,

$$FTE = \left( \frac{R_s}{R_{ss}} \right)^2 \frac{B_r(R_s, \theta_s, \phi_s)}{B_r(R_{ss}, \theta_{ss}, \phi_{ss})} \quad (1)$$

where,

$B_r$  – radial component of magnetic field

$R_s, R_{ss}$  – photospheric and source surface radii  
 $(\theta_s, \phi_s), (\theta_{ss}, \phi_{ss})$  – coordinates of the flux tube at the photosphere and the source surface.

An empirical relation between the solar wind velocity ( $V$ ) and the flux expansion factor has been obtained by Arge and Pizzo (1999) as:

$$V = 280.0 + 820.0 / (f^{(1.0/1.7)}) \quad (2)$$

This relation was obtained iteratively to match with the observed velocities at earth (see Arge and Pizzo, 1999 for details).

The technique of interplanetary scintillation (IPS) is capable of measuring out-of-ecliptic solar wind velocities within a heliocentric distance of 0.1 – 1.0 AU. The synoptic maps (v-maps) of solar wind obtained using the IPS data from Solar–Terrestrial Environment Laboratory (STELab), Nagoya University, Japan, has been used to study the global distribution of solar wind (Kojima et al., 1998). These studies and those using satellite data established that solar wind has two distinct components, the fast, with speed  $\sim 500 \text{ km s}^{-1}$ , and the slow, with speed  $\leq 450 \text{ km s}^{-1}$ , separated by a sharp latitudinal gradient. This was confirmed by the observations of high latitude solar wind by Ulysses during its fast latitude scan in 1994–95.

## 2 Present Work

Comparison of the v-maps and the latitudinal profiles of solar wind velocity obtained using IPS data acquired by STELab and NOAA/SEC version of Wang and Sheeley model, during rotations 1925–1927 in 1997.

A study of the latitudinal profile of solar wind velocity during solar maxima in 1989–1990 and 1998–1999 using:

- (a) NOAA/SEC version of the Wang and Sheeley model (source surface at  $2.5 R_{\odot}$ )
- (b) the potential field model of Hoeksema (source surface at  $3.25 R_{\odot}$ )

with an aim of predicting the latitudinal profile of the solar wind as would be seen by Ulysses in 2000, the maximum of the present solar cycle, when it passes the polar regions.

## 3 Data Used

- IPS data: from STELab, for three solar rotations CR 1925–1927, in 1997
- The photospheric magnetic field data used as input to the potential field model of:
  - NOAA/SEC version of Wang and Sheeley model: Mount Wilson Observatory
  - Hoeksema’s model: Wilcox Solar Observatory

## 4 Results

Figure 1: the v-maps of solar wind using the superposed data for three Carrington rotations CR 1925–1927, using:

- top panel: Wang and Sheeley model and the relation between flux expansion factor and the velocity in Eq. 2
- bottom panel: IPS data from STELab, after applying the technique of tomography

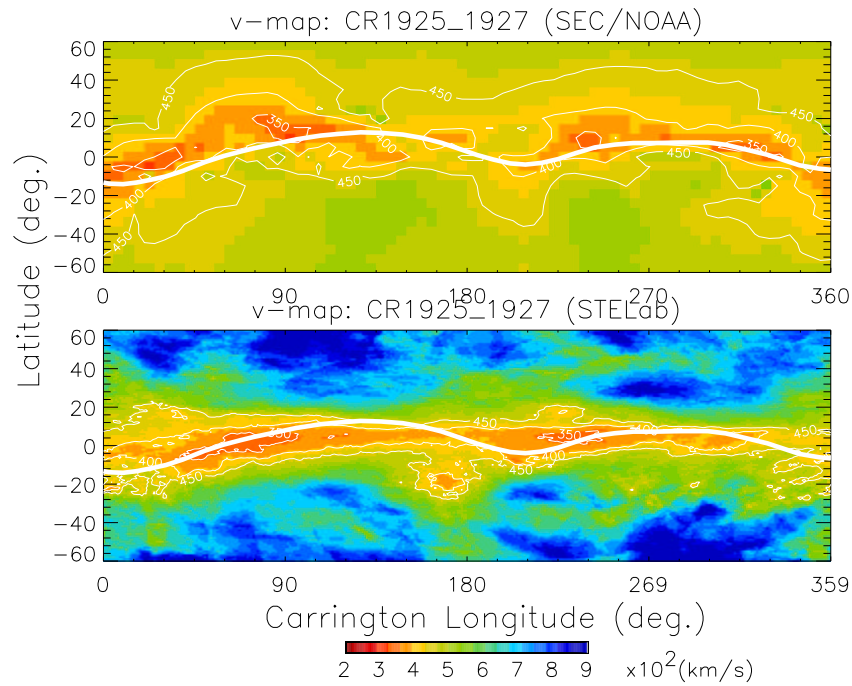


Figure 1:

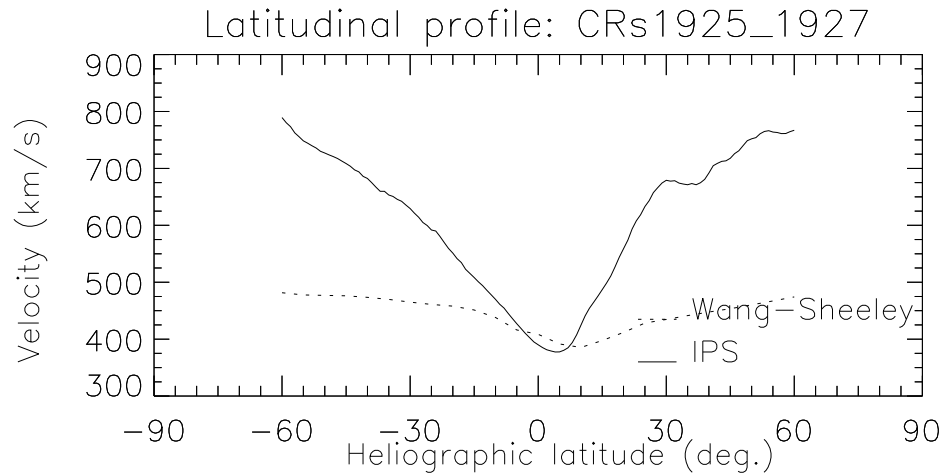


Figure 2:

to remove the bias caused in the estimation of velocity (Jackson et al., 1998, Kojima et al., 1998)

Superposed are the velocity contours of the slow solar wind at an interval of  $50 \text{ km s}^{-1}$ . The results show significant differences which will be discussed in the next section.

Figure 2: the latitudinal profile obtained from the above v-maps. Here, the solid line represents the wang and Sheeley model and the dashed line shows the IPS results.

Figure 3: the yearly averaged latitudinal profile of solar wind velocity in 1989, 1990 and 1998–99. These are solar maximum periods of the previous and ongoing solar cycle. The data are averages over the entire longitude.

- left panels: using NOAA/SEC version of Wang and Sheeley model (source surface, at  $2.5 R_{\odot}$ )
- right panels: the same, obtained using the

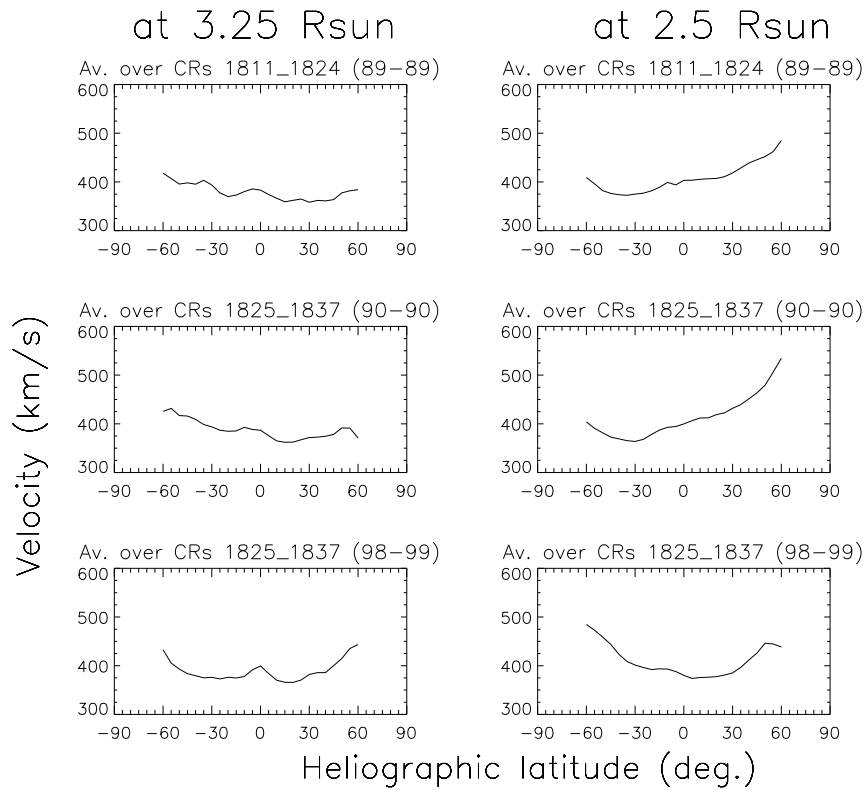


Figure 3:

potential field model of Hoeksema, (source surface, at  $3.25 R_{\odot}$ ).

In contrast to a well defined latitudinal gradient seen in Figure 2, during solar minimum, there is little variation with latitude during solar maximum periods shown in Figure 3. There

are differences between the results of the two models, Wang and Sheeley and Hoeksema. In the former, the velocity shows a larger gradient in the Northern hemisphere whereas in the latter, the slightly larger gradient, which is again less than that in the Wang and Sheeley model, is seen in the Southern hemisphere. Again, in the Wang and Sheeley model, the curve is a little skewed which is more pronounced in 1989 and 1990.

Cause of this discrepancy could be one or all of the following:

- Eq. 2 is calibrated for source surface at of  $2.5 R_{\odot}$ ; may not be valid at  $3.25 R_{\odot}$ .
- the polar fields may not be adequately corrected or taken care of in either WSO data or MWO data or both.
- the tilt of the solar rotation axis with respect to the ecliptic not being corrected.

## 5 Discussion of Figures 1 and 2

The v-maps in Figure 1 show the global distribution of solar wind on the source surface using NOAA/SEC version of Wang and Sheeley model and IPS observation. The location of the slow solar wind coincides in the two maps but the Wang and Sheeley model shows a larger latitudinal amplitude. Also, in the IPS results, the slow wind belt is rather flat and parallel to the equator but in the Wang and Sheeley model it is more sinusoidal. The striking difference is the absence of high speed wind in the Wang and Sheeley model which is very prominent in the IPS v-map. Listed below are the possible reasons for the apparent discrepancy (For a more detailed discussion see Bala, 1999).

1. Eq. 2 has been obtained iteratively, to match the observed velocities near the earth (see Arge and Pizzo, 1999, for details).

And this relation for the velocity at higher latitudes are not completely calibrated.

2. Potential field source surface model of Wang and Sheeley does not include the heliospheric current sheet. This will introduce uncertainty in the location of flux tubes beyond source surface distance (Wang and Sheeley, 1994). And that, perhaps, explains the broader slow solar wind and the absence of fast wind at high latitudes.
3. The north–south asymmetry seen in the Wang and Sheeley model in Figure 2 is partially due to the tilt of the solar rotation axis not being corrected in the observation. Note that there is a north–south asymmetry in the IPS data as well.
4. The IPS data are obtained within a heliocentric distance of 0.1 – 1.0 AU. To prepare the v-maps the velocities are mapped back to source surface along the Archeme-

dian spiral, assuming radial flow, using the relation:

$$\begin{aligned}\Phi_0 &= \Phi_R + \frac{R\Omega}{V_R} \\ \Theta_0 &= \Theta_R\end{aligned}\quad (3)$$

where,  $\Phi_0$  and  $\Phi_R$  are the longitudes, and  $\Theta_0$  and  $\Theta_R$  the latitudes, on the source surface and at a distance  $R$  from the Sun, respectively.  $\Omega$  is the angular speed of solar rotation. This equation does not handle the radial acceleration of the solar wind within  $30 R_\odot$  nor does it include stream–stream interaction during its transit from Sun to earth. Also, it neglects non-radial emission of plasma. The source surface is situated within the “acceleration region” and therefore, application of the above equation would introduce some error in the velocities obtained at the source surface and thereby, in the v-map.

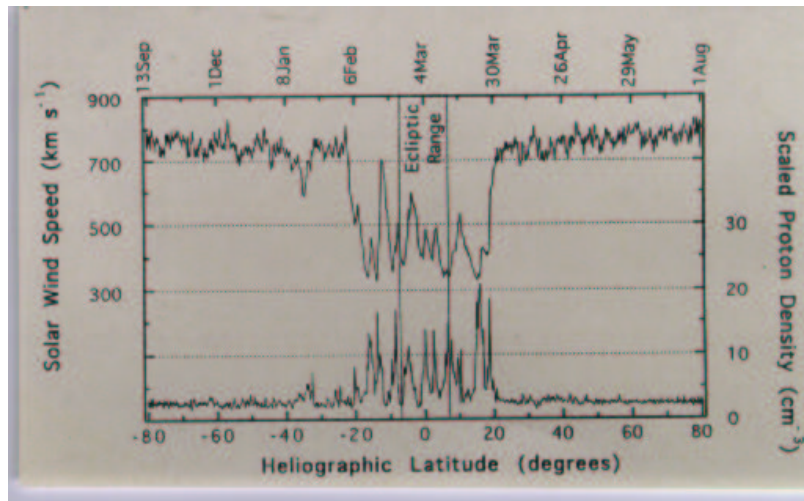


Figure 4:

## 6 Earlier Works

Figure 4 shows the latitudinal profile of solar wind velocity observed by Ulysses during the fast latitude scan in 1994–95, a period of low solar activity. Note the sharp latitudinal gradient in velocity. The latitudinal profiles depicted in Figure 2, especially, the one using IPS data, are in agreement with the Ulysses observation.

Earlier, in a study using IPS data of solar

## 7 Concluding Remarks

The NOAA/SEC version of Wang and Sheeley model could be used to study the global distribution of solar wind at source surface. This model is important as there is no existing way of observing solar wind as close to the Sun as  $2.5 R_{\odot}$ . However, the model as well as the relationship between flux tube expansion factor and solar wind speed at 1 AU need to be improved as discussed in Section 5.

The latitudinal profiles shown in Figure 3 is an average over longitude. Our results agrees very well with that of Rickett and Coles (1991), which is also longitudinally averaged. This average structure is what Ulysses will be observing in 2000. However, it is important to see the latitudinal profile at different longitudinal bands since magnetic field need not be uniform along the azimuth. Such a study is currently underway.

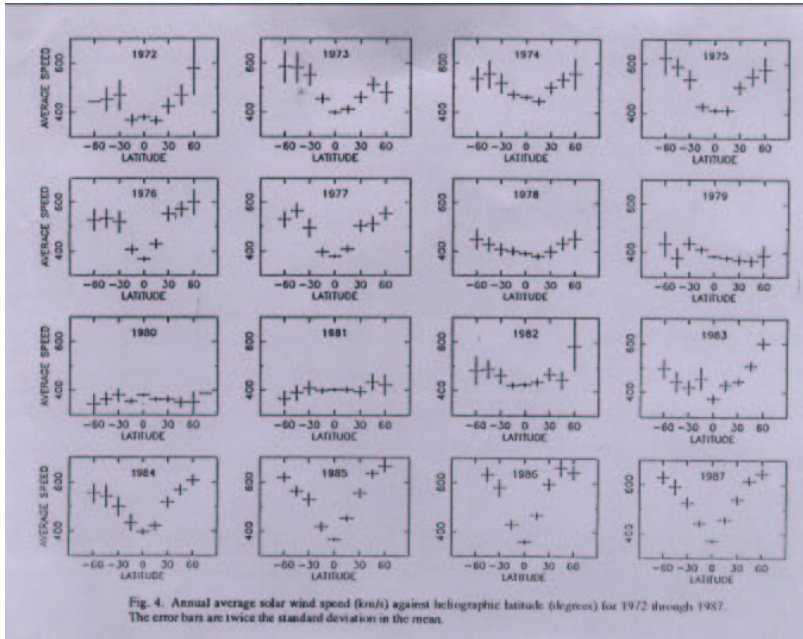


Figure 5:

wind velocity, Rickett and Coles (1991) have shown that there was little latitudinal gradient during solar maximum. On the other hand, an increase in speed with latitude in both the hemispheres was very prominent during solar minimum (Figure 5). The present results (Figure 3) are very much in agreement with the results of Rickett and Coles.



## Acknowledgements

Thanks are due to Drs. V. J. Pizzo and C. N. Arge, SEC, NOAA, Boulder, CO, for providing the data from their Wang and Sheeley model (visit <http://sec.noaa.gov/~narge/> for synoptic maps) and Dr. J. T. Hoeksema, Stanford University, for the spherical harmonic coefficients necessary for the present study. One of the authors (BB) wishes to express her gratitude to Dr. M. Kojima for providing with the IPS data and many discussions.

## Literature Cited

- Arge, C. N. and V. J. Pizzo, 1999: *Journal Geophys. Res.* (in Press)
- Bala B., 1999: *Solar Phys.* (in Press)
- Wang, Y.-M. and N. R. Sheeley, 1994: *Journal Geophys. Res.* **99**, 6597.

- Jackson, B. V., P. L. Hick, M. Kojima, and A. Yokobe, 1998: *Journal Geophys. Res.* , **103**, 12049.
- Kojima, M., M. Tokumaru, H. Watanabe, A. Yokobe, K. Asai, B. V. Jackson, and P. L. Hick, 1998: *Journal Geophys. Res.* , **103**, 1981.
- Phillips, J. L., S. J. Bame, A. Barnes, B. L. Barraclough, W. C. Weldman, B. E. Goldstein, J. T. Gosling, G. W. Hoogeveen, D. J. McComas, M. Neugebauer and S. T. Suess, 1997: *Geophys. Res. Lett***22**, 3301.